

Vibro Stone Column Installation and its Effect on Ground Improvement

F. Kirsch

Dr.-Ing., GuD Geotechnik und Dynamik Consult GmbH, Berlin, Germany

ABSTRACT: Results of installation accompanying measurements of the in situ stresses, the ground stiffness and the ground surface vibrations in various test fields are presented. Following the installation the stone columns are subjected to group loading whilst the instrumentation remains active including load pressure cells and settlement transducers. The results show significant alteration of the stress state and the soil stiffness during penetration of the depth vibrator and the subsequent stone column installation. Two major effects can be distinguished: the displacement of the ground due to the creation of the stone column body and the ground vibration with associated changes within the soil due to the movements of the depth vibrator. The results of the measurements are used to model the installation effects in numerical analyses using the finite element method. Comparison between the numerical results and the findings of the measurements as well as the load test results are used to calibrate this numerical model. Finally parametric studies are undertaken to estimate the additional improvement effect of the installation process on the total ground improvement factor for vibro stone column measures

1 INTRODUCTION

Developed in the 1950ies as an extension of the at that time well established vibratory ground improvement method the first vibro stone column project is believed to be the foundation measure for a locomotive shed in Braunschweig, Germany (Kirsch 1993). Since that time depth vibrators are used to install stone columns in cohesive soils by displacing and if possible compacting the in situ soil.

Usually the fields of application of vibro stone columns and deep vibratory ground improvement are distinguished depending on the grain size distribution of the soil. It is apparent that there is no distinct partition but a range in which densification of the soil is still possible, but additional material is usually added to ensure an effective and economical improvement.

Generally it is assumed that the surrounding soil maintains its original strength and stiffness parameters whilst the improvement is dominated by the highly compacted stone column material. Any improvement of the in situ soil acts as a hidden safety in the system.

The design of vibro stone column measures does not take into account the improvement of the surrounding soil apart from a certain increase in the stress state typically using earth pressure at rest assumptions. Furthermore the design parameters such

as stiffness and shear strength are derived from investigations prior to the column installation and are usually not crosschecked with additional testing.

On the other hand it is known from experience that one can measure a significant loss of cone penetration resistance immediately after the stone column installation and a subsequent rise often above original values after some time. Therefore it is deemed necessary to put focus on the investigation of alterations in the soil properties during vibratory stone column installation in order to draw a realistic picture of their load carrying behaviour

2 MEASUREMENTS DURING STONE COLUMN INSTALLATION

2.1 *Ground movement*

It is apparent that the installation of a grid of stone columns in mainly uncompactible soils results in a significant surface heave, which was monitored e.g. by Gruber (1994). He reports that the volume of the surface heave was between 90% and 100% of the installed stone column volume. Figure 1 shows the surface heave after the installation of five 0.8 m diameter stone columns in a 1.6 m diagonal grid. One should keep in mind that the influence on the stress state becomes essential when this movement is restrained e.g. by a stiff layer on top.

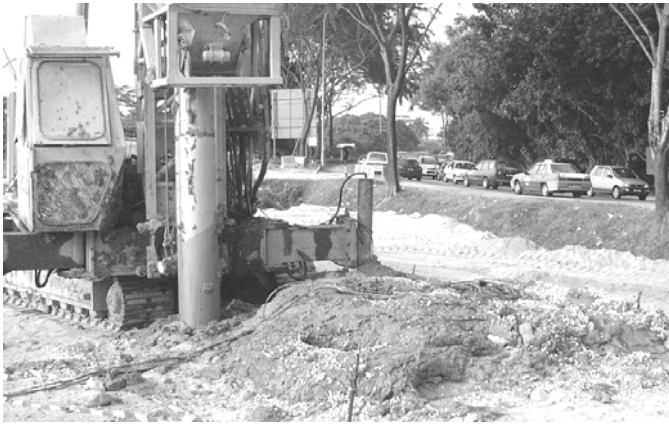


Figure 1. Surface heave after the installation of five 0.8m diameter stone columns.

2.2 In situ stresses

Measurements of the stress field surrounding vertical displacement elements such as piles or stone columns are reported by many authors. Whilst Gruber (1994) reports no significant increase of the horizontal stresses after the installation of stone columns, Watts et al. (2000) show an increase of up to 60 kPa of the horizontal stresses during column installation. Randolph et al. (1979) gave an explanation of the processes during pile driving within the framework of critical state soil mechanics during cavity expansion, which was used by Cunze (1985) to predict the increase in pore water pressure due to pile driving.

The development of additional stresses due to stone column installation was addressed by Jacobi (1998) using simple but effective measurement devices to find, that the installation of three vibro stone columns in front of the gauge leads to additional stresses in a silty soil of up to 100 kPa as shown in figure 2.

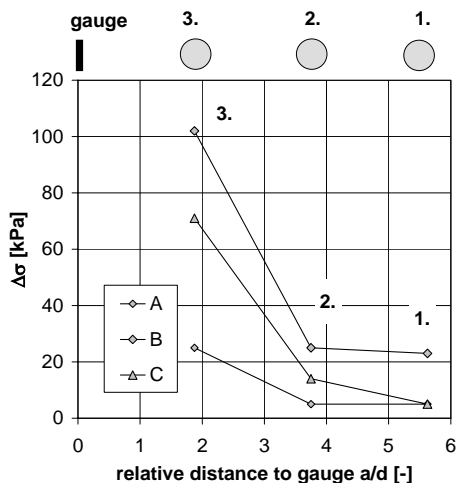


Figure 2. Increase of total stresses due to the subsequent installation of three stone columns with a diameter $d = 0.8$ m in falling distance a to the gauge for three different series A, B, C.

The results of pore pressure measurements during the installation of stone columns in two test fields each consisting of 25 columns in a square pattern were presented by Kirsch (2004). Figure 3 shows the outline of the test fields.

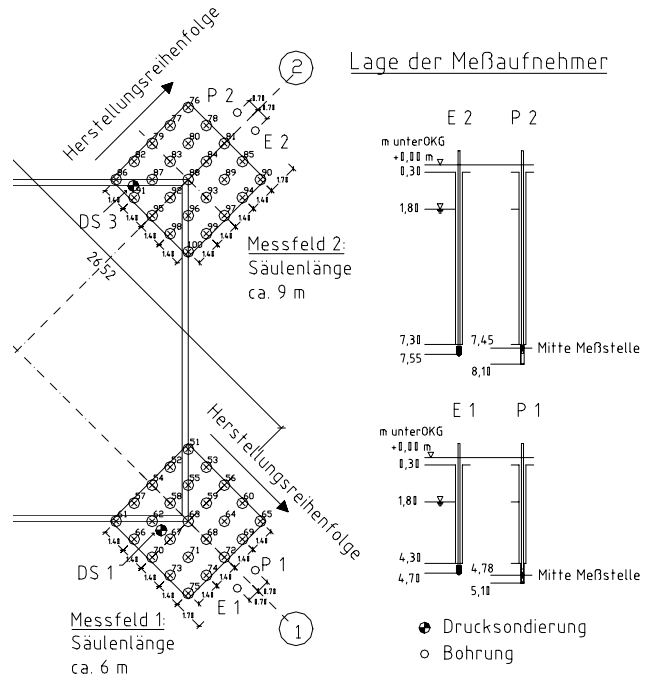


Figure 3. Outline of test fields 1 and 2.

The earth and pore water pressure cells (E1 and E2) and the Ménard pressuremeters (P1 and P2) were set up prior to the column installation. The installation sequence was chosen moving towards the measurement devices.

The comparison between the predicted (according to Cunze 1985) and the measured pore water pressure increase due to the stone column installation is shown in figure 4. Apart from a reasonable match, it becomes apparent, that there is a considerable scatter in the results.

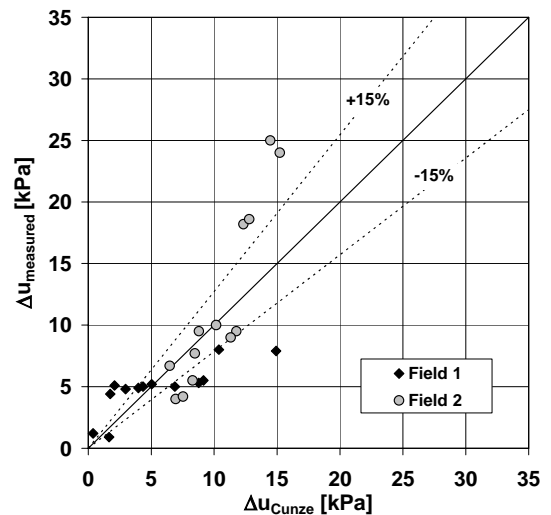


Figure 4. Measured and predicted pore water pressure increase.

Looking at the stress development during the installation of each single column within the above test fields one can distinguish different phases: 1-Lowering of the vibrator, 2-alternating lift and sag cycles compacting the stone fill supported by air pressure, 3-stop to refill the material lock inside the vibrator (see figure 5).

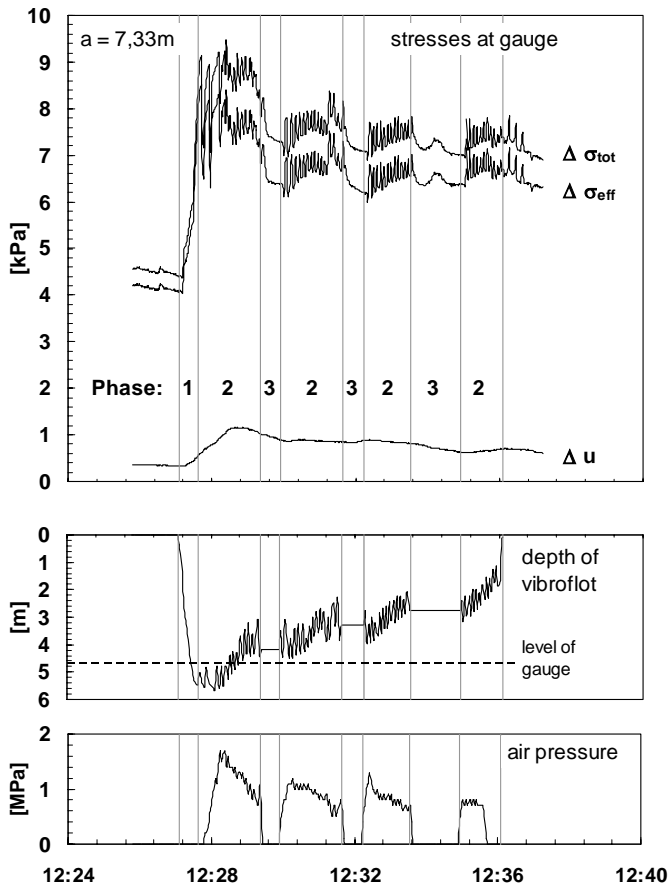


Figure 5. Additional horizontal stresses and pore water pressures at a depth of 4.7 m during the installation of a stone column ($d = 0.8$ m) in a distance of $a = 7.33$ m.

The example shown in figure 5 depicts the total horizontal stresses measured in a distance of 7.33 m in a depth of 4.7 m and the effective horizontal stresses calculated by subtraction of the measured pore water pressures during the installation of a stone column having 0.8 m diameter and a length of approx. 5.5 m. Thus the gauge was installed in weak to stiff sandy silt of medium plasticity (MI). Obviously the maximum stress peak is reached, when the depth of the vibrating tip of the vibrator reaches the level of the gauge. The lift and sag cycles invoking the lateral displacement of the stone column material can be easily identified in the stress development. After completion of the stone column the stress state both in terms of pore water pressure and effective stresses remains higher than before column installation.

Horizontal stress increases at a given point measured during the installation of the whole group of 25 columns in each of the two test fields are shown in figure 6. Displayed are the effective horizontal stresses in relation to the initial stresses and normalized by the vertical overburden pressure leading to a specific k -value. Also shown is the installation sequence with locations of the column installation getting closer to the place of the gauges.

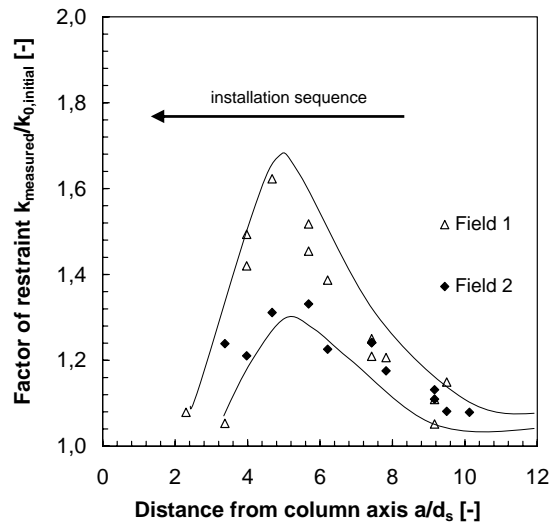


Figure 6. Factor of restraint measured during the installation of stone columns ($d_s = 0.8$ m).

It becomes evident that the stress state rises to a value of up to 1.6 times the initial stresses due to the ground displacement when the location of column installation gets closer to the measurement location. Once a critical distance of about four to five times the column diameter d_s is reached the displacing virtue is superimposed by stress reducing effects which can be addressed as remoulding and dynamic excitation leading to a considerable loss of strength.

2.3 Stiffness development

Looking at the development of the in situ stiffness the above test fields were also instrumented with pressuremeter cells in each of the two fields. Figure 7 shows the measured Ménard-moduli in relation to the distance from the latest installed column with an installation sequence approaching the pressuremeter cell.

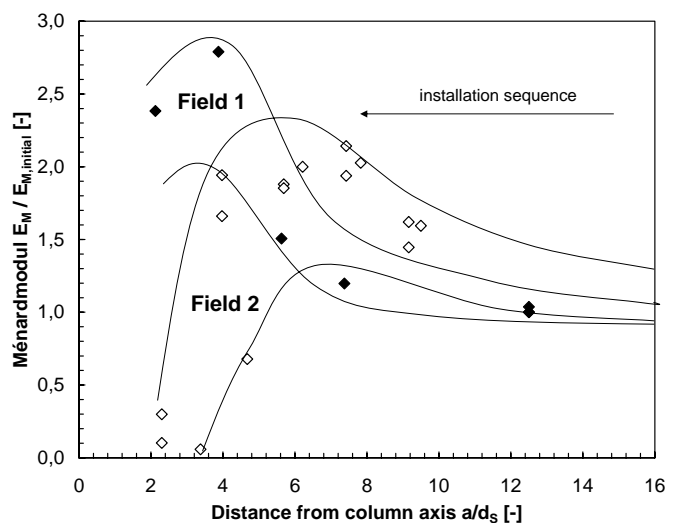


Figure 7. Development of ground stiffness during the installation of stone columns ($d_s = 0.8$ m).

We find that the stiffness rises to a maximum of 2.5 times the initial stiffness in a distance of about 4 to 5 times the column diameter d_s . Installation of stone columns closer than $4 \cdot d_s$ lead to a loss of stiffness even below initial stiffness showing a potential liquefaction of the soil due to the dynamic excitation.

2.4 Ground vibration

We found that there is a critical distance from the location of the column installation of approximately five times the column diameter. This distance corresponds to the distance where the dynamic excitation of the soil rises rapidly following an exponential law. Figure 8 shows the typical response of the ground surface to the excitation of a depth vibrator during the installation of a stone column. In figure 9 the maximum particle velocity is drawn as a function of the distance to the column axis normalized by the column diameter.

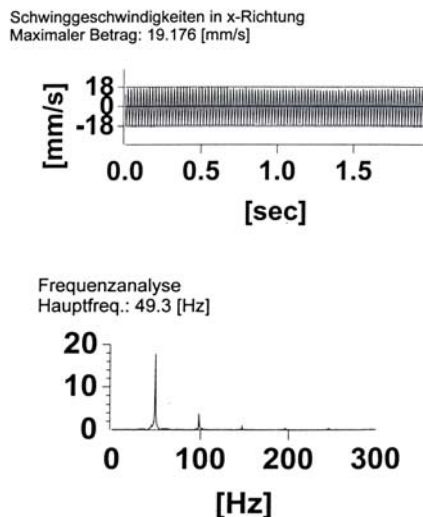


Figure 8. Typical signal of ground vibration induced by stone column installation (z: vertical).

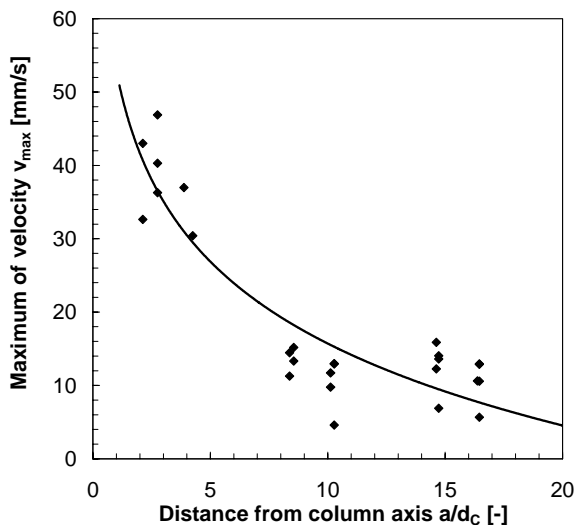


Figure 9. Maximum particle velocity v_{max} at ground level during the installation of vibro stone columns ($d_c = 0.8m$) at a distance a [m].

2.5 Summary of installation effects

Summing up we can distinguish different effects:

- Stress and stiffness increases in the surrounding soil due to vibro stone column installation can be verified by in situ measurements.
- These increases can be expected to be permanent in soils which do not tend to creep, i.e. having a significant fraction of sandy soil.
- The soil adjacent to the column is displaced and remoulded during column installation.
- The soil displacement leads to an increase in the stress state and the stiffness in a distance between $4 \cdot d_c$ and $8 \cdot d_c$ around the columns and the column group respectively.
- Dynamic excitation close to the column reduces stress and stiffness increases.

These findings have important impact on stone column design and practical application.

- Installation effects should be included in design and analysis in order to model the behaviour under loading correctly.
- Due to the stress increase vibro stone column installation influences existing structures within a distance of approx. 8 to 10 times the column diameter.
- The rise of the stress level is reduced within a distance of less than 4 times the column diameter due to remoulding and liquefaction effects.
- Column installation in the direct vicinity to sensitive structures should always be by moving towards the structure.

3 SIMULATION OF INSTALLATION EFFECTS

3.1 Methodology

There are a couple of attempts published in literature to simulate the effects which are induced by a depth vibrator in the soil (e.g. Fellin 2000). Due to the complexity of the associated phenomena the models used are rather simple in terms of geometrical conditions. Schweiger (1989) applies a strain field in order to model the volume input of column installation. Most authors model the displacing effect of column installation by the a cylindrical cavity expansion starting from an arbitrary diameter to the final column (e.g. Debats et al. 2003).

In the following chapters the individual effect of simulating a cavity expansion in the numerical model is shown. Additionally the above finding of an enhancement zone in the far field as a global installation effect is introduced in the analysis to come to a numerical procedure which accounts for installation effects of a group of stone columns. Figure 10 illustrates the two main installation effects of vibro stone columns.

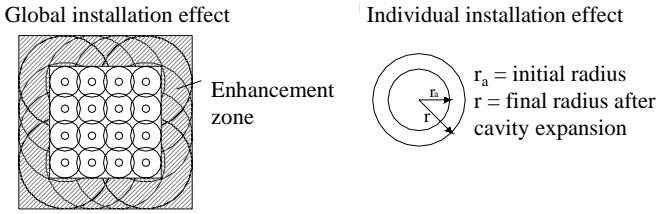


Figure 10. Global and individual installation effect of vibro stone column ground improvement.

3.2 Cavity expansion

To show the effects incorporated in the modelling of a cylindrical cavity expansion the installation of a single stone column in a layered soil is modelled in a 3-D elasto-plastic continuum. Table 1 shows the material data, whilst the finite element model is shown in figure 11. In order to avoid singularities the cavity expansion close to the column toe starts with a zero expansion rising to the chosen value within the first three elements above the column toe.

Table 1. Soil parameters for cavity expansion example.

Layer	Depth [m]	E [kPa]	ϕ' [°]	c' [kPa]	ν [-]	ψ [°]	γ [kN/m ³]
1	0-3	500	10	15	0.3	0.3· ϕ	9.0
2	3-7	750	10	15	0.3	0.3· ϕ	9.0
3	7-10	1000	10	15	0.3	0.3· ϕ	9.0
4	10-20	1500	10	15	0.3	0.3· ϕ	9.0

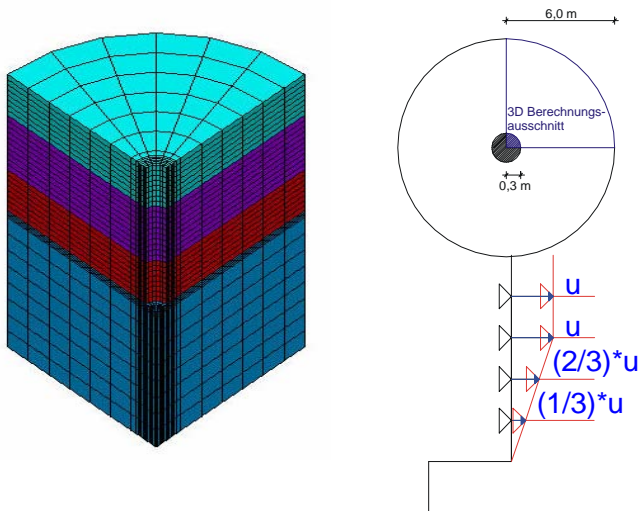


Figure 11. 3-D FE model for cavity expansion.

The expansion starts from a initial radius of the column of 0.3m. Figure 12 shows the plots of radial stresses σ_x , radial displacements u_x and plastic strains ϵ_{pl} due to a cavity expansion of 0.1 m radius amplification. In Figure 12 the radial stresses in a radial slice in a depth of 3 m in soil layer 2 are plotted for two exemplary radius magnifications of $a = 0.01$ m and $a = 0.15$ m. According to Baguelin et al. (1978) the stress increase in an elasto-plastic medium due to cavity expansion can be calculated as:

$$\sigma_{rr} = (\sigma_F + c \cdot \cot(\phi)) \cdot \left(\frac{G}{(\sigma_{h0} + c \cdot \cot(\phi)) \cdot \sin(\phi)} \cdot \frac{(r_0 + a)^2 - r_0^2}{(r_0 + a)^2} \right)^{\frac{1-K_a}{2}} - c \cdot \cot(\phi) \quad (1)$$

with

$$\sigma_F = \sigma_{h0} \cdot (1 + \sin(\phi)) + c \cdot \cos(\phi)$$

$$K_a = \frac{1 - \sin(\phi)}{1 + \sin(\phi)}$$

With the above parameters from table 1 we calculate:

- $a=0,01$ m: $\sigma_{rr}=\sigma_x=28$ kPa,
- $a=0,15$ m: $\sigma_{rr}=\sigma_x=71$ kPa.

These values correspond reasonably well with the calculated values in figure 13. The deviation results from the fact, that in the numerical analysis a non-associated flow rule is incorporated using the angel of dilatancy ψ .

There are other possibilities to model the stress increase in the soil e.g. the application of a temperature gradient to the column material in addition to the definition of a temperature expansion coefficient or the application of a strain or a stress field to the finite element net. Kirsch (2003) showed that the cavity expansion described here is superior to the other methods due to numerical stability.

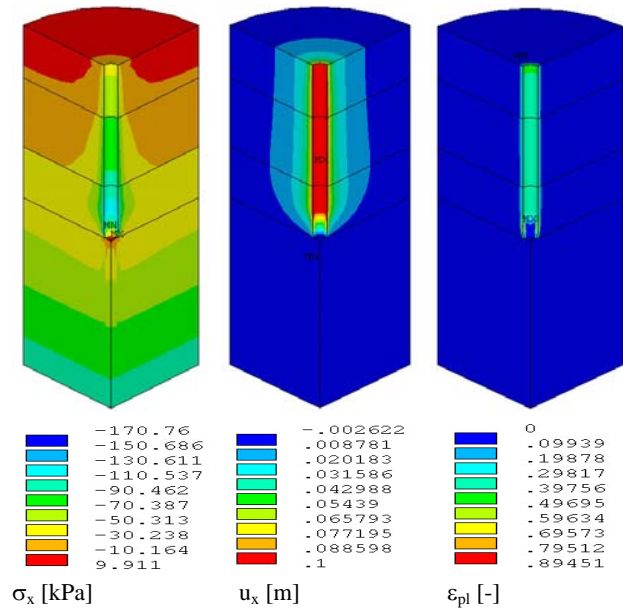


Figure 12. Radial stresses σ_x , radial displacements u_x and plastic strain ϵ_{pl} .

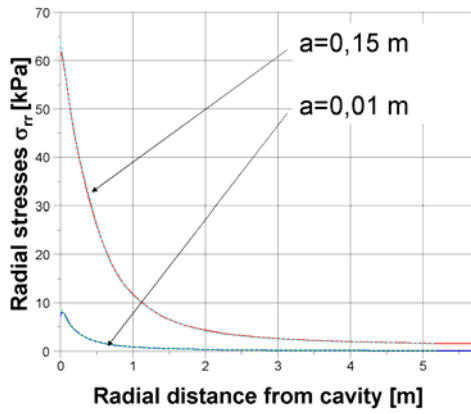


Figure 13. Radial stresses σ_x in relation to the distance from the cavity surface for an expansion of 0.01 m and 0.15 m respectively.

3.3 Global and individual installation effects and the influence on the ground improvement

In addition to the above examined cavity expansion and in order to model the soil displacing effects of vibro stone column installation with subsequent stress increase we learnt from the in situ measurement that there exists an enhancement zone around a column or a column group respectively. In the numerical model this zone is defined by two distances b_1 and b_2 from the outmost column centre as shown in figure 14.

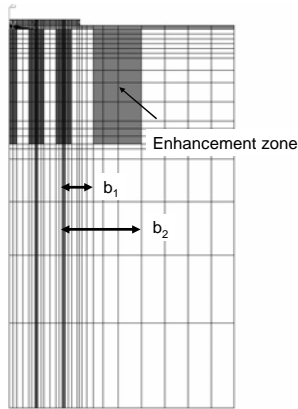


Figure 14. Enhancement zone in the numerical model.

To illustrate the effect of a stiffness increase in the enhancement zone it is necessary to take a look at the load settlement behaviour of the column group and vary the stiffness in the enhancement zone. Therefore the situation shown in figure 15 shall be simulated, which corresponds to the test field as presented in the previous chapter. A group of 25 columns in a layered soil is loaded by a square shallow foundation of $B = 7.2$ m up to 180 kPa. The improvement due to vibro stone columns is defined by the improvement factor β being a settlement reduction factor. The additional improvement due to stiffness increase $f = E/E_{init}$ is defined by β^* , whilst the additional improvement due to the cavity expansion a is denominated as β^{**} .

$$\beta = \frac{S_{\text{without improvement}}}{S_{\text{with improvement}}} ; \quad \beta^* = \frac{S_{\text{with improvement}}(a=0, f=1)}{S_{\text{with improvement}}(a=0, f>1)} ; \quad (2)$$

$$\beta^{**} = \frac{S_{\text{with improvement}}(a=0, f=1)}{S_{\text{with improvement}}(a>0, f=1)}$$

The results of the numerical simulation in terms of the load settlement response are shown in figure 16. Eight different situations are analysed: The original situation without ground improvement by vibro stone columns; Vibro stone column improved soil beneath the footing without the simulation of installation effects neither individual (cavity expansion $a=0$) nor global (enhancement zone, $f=1$) and six computations with different stiffness increase factors $f=1.33 \dots 3.0$ in the enhancement zone with $b_1=2 \cdot d_C$, $b_2=5 \cdot d_C$ to model the global installation effect. The resulting improvement factors β from eq. (2) are shown in figure 17, whilst the improvement factors β^* from eq. (2) are shown in figure 18.

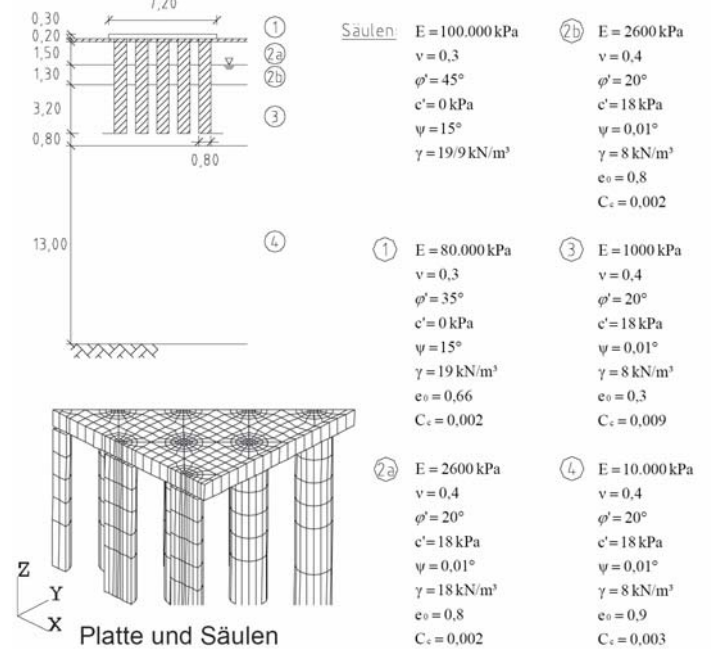


Figure 15. Geometry and parameters of the test field.

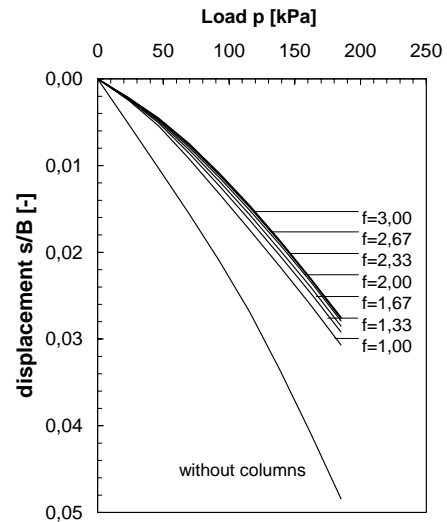


Figure 16. Load settlement response of the square footing ($B = 7.2$ m) considering global installation effects for different stiffness increase factors.

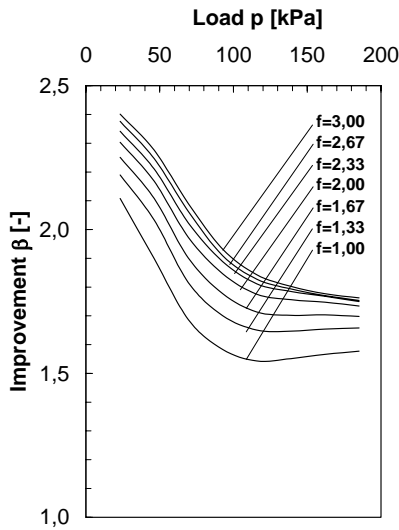


Figure 17. Improvement factor β as defined in eq. 2 for different stiffness increase factors f in the enhancement zone.

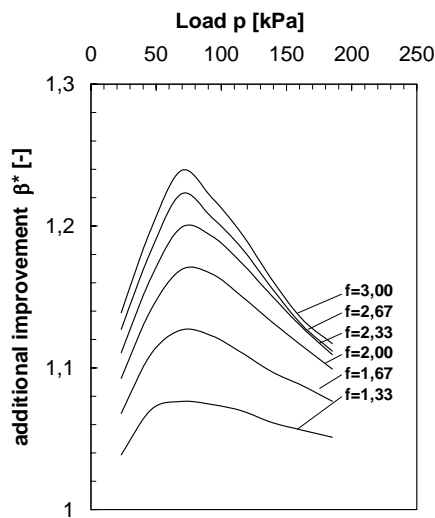


Figure 18. Improvement factor β^* as defined in eq. 2 for different stiffness increase factors f in the enhancement zone.

Obviously the improvement factor due to the global installation effect with a stiffness increase in the enhancement zone is dependant on the loading state, which can be explained by the fact, that at higher loadings the plastic deformation plays a predominant role and stiffness increase has a minor influence. Depending on the stiffness increase factor the additional improvement β^* reaches values of up to 1.25, meaning that the consideration of the global installation effects leads to a rise in the calculated improvement of 25% of the calculated improvement factor without taking into account any installation effects.

So far we only incorporated the global installation effect. Now we take a look at the influence of the individual installation effect being the cavity expansion as presented in chapter 3.2. We analyse the same situation from the test field.

Figure 19 shows the load settlement response of the square footing for situations without ground improvement stone columns, with columns however only considering the individual installation effect by applying a cavity expansion a of 0%, 2%, 4% and

8% of the final column diameter $d_c=0.8\text{m}$. Figures 20 and 21 depict the corresponding improvement factors β and β^{**} from eq. (2).

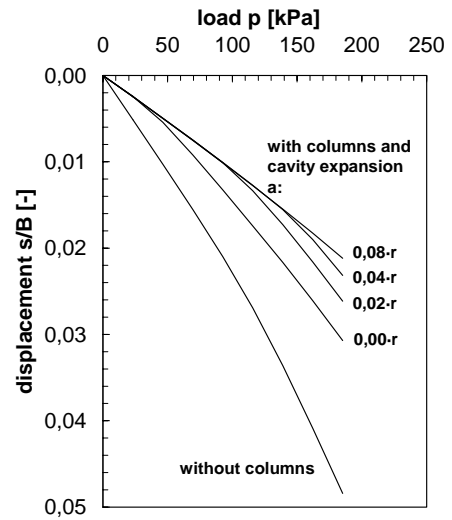


Figure 19. Load settlement response of the square footing ($B = 7.2 \text{ m}$) considering individual installation effects for different cavity expansion values a .

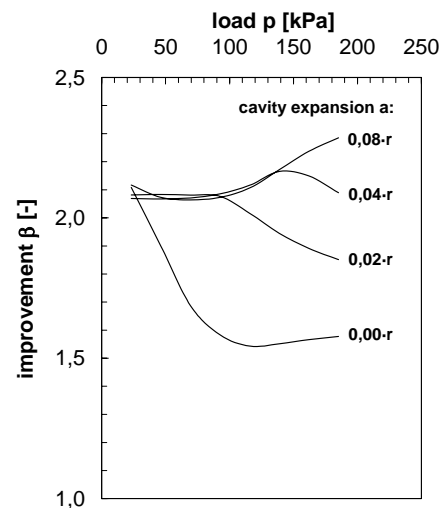


Figure 20. Improvement factor β as defined in eq. 2 for different cavity expansion values a for each column.

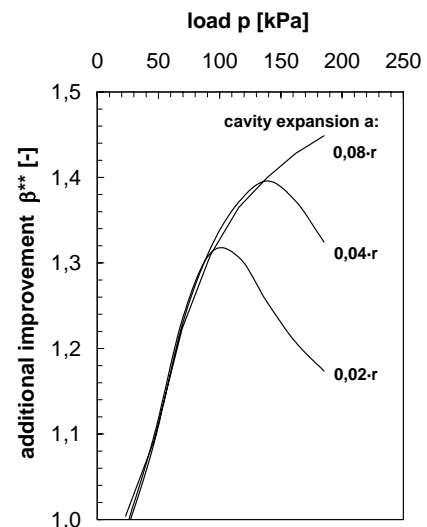


Figure 21. Improvement factor β^{**} as defined in eq. 2 for different cavity expansion values a for each column.

It turns out that the consideration of the individual installation effect by applying a cavity expansion between 0% and 8% of the final column diameter leads to additional improvement factors of up to 45% of the improvement without any installation effects. The additional improvement is highly dependant on the loading stage rising with higher loading and falling again after reaching a maximum at loading values which are again dependant on the cavity expansion value. This behaviour can be explained by taking into account the nature of the load carrying mechanisms of stone columns. At early loading stages the stone column material reaches its plastic limit and the column starts to bulge causing lateral support in the ground. The higher the initial horizontal stress state, which is influenced by the value of the cavity expansion, the better this lateral support prevents the column from bulging leading to reduced settlements. Once the limit state in the surrounding soil is reached this additional support plays a minor role leading to lower additional improvement factors at higher loading stages.

This explains that both individual and global installation effects play a positive role by reducing the settlements under load, but do not influence the ultimate load of the structure. This effect can be compared with prestressing in reinforced concrete. To illustrate this effect figure 22 shows the load settlement response of a single column $d_C = 1.0$ m loaded by a circular plate $d = 2.0$ m.

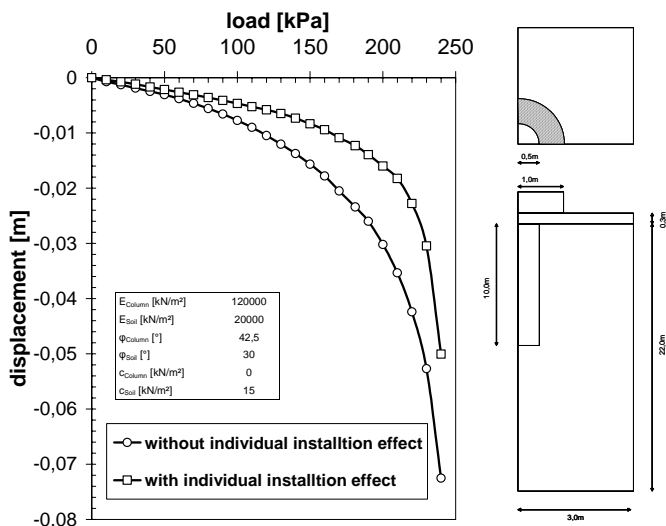


Figure 22. Calculated load settlement response of a single column with and without the consideration of installation effects.

3.4 Comparison with analytical design

The measurements in the above described test fields gave reason to set the cavity expansion to model individual installation effects to a value of $a = 4\%$ of the final column diameter of $d_C = 0.8$ m in order to match the stress increase surrounding the column. The stiffness increase factor accounting for global installation effects was measured as $f = 2.0$ in a zone

limited by $b_1 = 2 \cdot d_C = 1.6$ m and $b_2 = 5 \cdot d_C = 4.0$ m around the column group.

In order to judge the results of the numerical analysis a comparison is made with the results of analytical design methods. Priebe (2003) allows the computation of settlements of a stone column group in a floating situation meaning that the columns are not necessarily set on a hard layer. The routine of Goughnour and Bayuk (1979) was extended by Kirsch (2004) to calculate the settlements of a group of columns. Both methods are compared with the calculated load settlement response in figure 23.

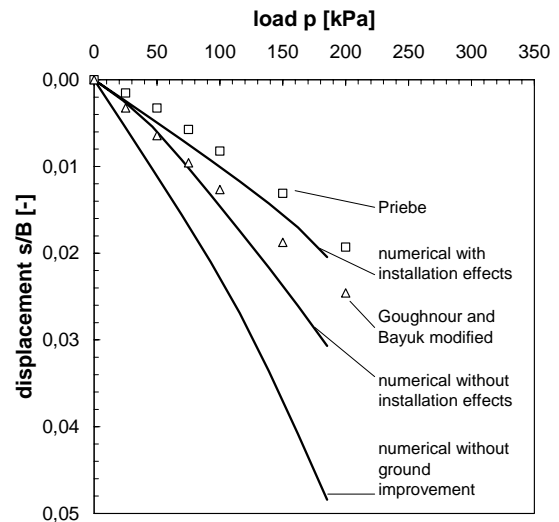


Figure 23. Analytical and numerical results of the load settlement behaviour of a group of 25 stone columns.

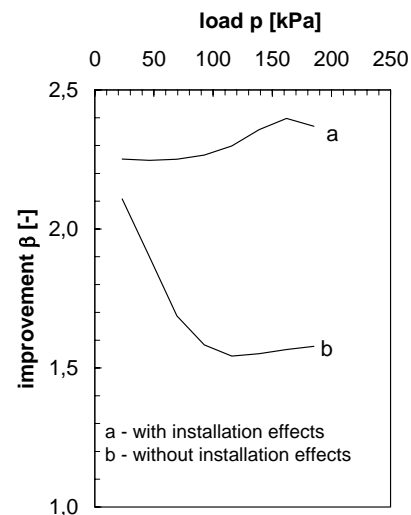


Figure 24. Improvement factor β for the with and without the consideration of installation effects in the numerical analysis.

It can be seen that the assumptions made in analytical procedures about the horizontal stress ratio chosen as $k=1$ gives a reasonable picture of the actual situation. Therefore both the method of Priebe (2003) and the method of Goughnour and Bayuk (1979) with the modification by Kirsch (2004) are able to predict the settlements with reasonable accuracy.

The consideration of installation effects in numerical analysis leads to a steady distribution of the improvement factor β along the different loading stages as shown in figure 24.

4 SUMMARY AND CONCLUSIONS

The extensive instrumentation of two test fields each consisting of 25 vibro stone columns allowed the assessment of the influence of the stone column installation on the soil properties.

Two effects can be distinguished. An individual installation effect causing the rise of the stress state and a global installation effect in an enhancement zone around the columns and the column group respectively.

Both effects can be modelled numerically making use of analogical procedures such as the cavity expansion and the stiffness increase.

The isolated and combined analysis of the additional improvement due to the installation effects showed that within a group of 25 columns the consideration of the global installation effect raises the improvement by approx. 5% to 25% whilst the individual installation effects raise the improvement to values about 40% higher than without installation effects. The combination of both the global and the individual installation effect leads to a more steady distribution of the improvement along the different loading stages.

REFERENCES

- Antoine, P.C. et al. 2003. Study of deep compaction in order to its application to deep foundations. *Proc. 13th Europ. Conf. Soil Mech. Geotech. Engg.* Vol 2: 443-448.
- Baguelin, F. et al. 1978. *The Pressuremeter and Foundation Engineering*. TransTech Publications.
- Cunze, G. 1985. *Ein Beitrag zur Abschätzung des Porenwasserüberdruckes beim Rammen von Verdrängungspfählen in bindigen Böden*. Dissertation. Uni Hannover.
- Fellin, W. 2000. *Rütteldruckverdichtung als plastodynamisches Problem. Advances in geotechnical engineering and tunneling 2*. Rotterdam: Balkema.
- Goughnour, R.R and Bayuk, A.A. 1979. Analysis of stone column - soil matrix interaction under vertical load. *Coll. Int. Renforcements des Sols*. Paris. 279-285.
- Gruber, F.J. 1994. *Verhalten einer Rüttelstopfverdichtung unter einem Straßendamm*. Dissertation. TU Graz.
- Jacobi, C. 1998. *Kurzbericht Hildesheim Wohnbauung Pieperstraße*. unpubl.
- Kirsch, F. 2003. *Die numerische Analyse von Baugrundverbesserungsmaßnahmen, 2. Zwischenbericht, IGB-TUBS*, unpubl.
- Kirsch, F. 2004. *Experimentelle und numerische Untersuchungen zum Tragverhalten von Rüttelstopfsäulengruppen*. Dissertation. TU Braunschweig.
- Kirsch, F. et al. 2004. Berechnung von Baugrundverbesserungen nach dem Rüttelstopfverfahren. In DGGT (ed.), *Vorträge der Baugrundtagung 2004 in Leipzig*. 149-156. Essen. VGE.
- Kirsch, K. 1993. Die Baugrundverbesserung mit Tiefenrüttlern. In K. Englert & M. Stocker (eds.), *40 Jahre Spezialtiefbau*: 219-255. Düsseldorf: Werner.
- Priebe, H. 2003. Zur Bemessung von Stopfverdichtungen - Anwendung des Verfahrens bei extrem weichen Böden, bei schwimmenden Gründungen und beim Nachweis der Sicherheit gegen Gelände- oder Böschungsbruch. *Bautechnik* 80. 380-384.
- Randolph, M.F. et al. 1979. Driven piles in clay - the effects of installation and subsequent consolidation. *Géotechnique* 29. No. 4: 361-393.
- Schweiger, H.F. 1989. *Finite Element Analysis of Stone Column Reinforced Foundations*. Dissertation. University of Swansea.
- Watts, K.S. et al. 2000. An instrumented trial of vibro ground treatment supporting strip foundations in a variable fill. *Géotechnique* 50. No. 6: 699-708.